Wall-induced Cross-field Electron Transport with Oblique Magnetic Field Lines

IEPC-2013-077

Presented at the 33rd International Electric Propulsion Conference,
The George Washington University, Washington, D.C., USA
October 6–10, 2013

Jan Miedzik* and Serge Barral†
Institute of Plasma Physics and Laser Microfusion, 01-497 Warsaw, Poland

and

Stéphan Zurbach‡
Snecma, Safran Group, 27208 Vernon, France

Abstract: A quasineutral Particle-In-Cell model with guiding center approximation of electrons motion (PIC-GC-electron/PIC-ion) is employed to assess the influence of tilted magnetic field lines on electrons transport across magnetic field lines. Computations along a single magnetic field line suggest that highly ion focusing topology increases electrons cross-field drift and that a significant increase of electron temperature isotropisation muste

Nomenclature

$\mathbf{B}$, B	= magnetic field (vector, magnitude)
e	= absolute electron charge
$E_{\parallel}$	= electric field along $\mathbf{B}$
f_v	= electron velocity distribution function
f_ε	= electron energy distribution function
m_e	= electron mass
m_i	= ion mass
n_n	= density of neutrals
N_α	= number of particles of species α ($\alpha = n$: neutrals, $\alpha = e$: electrons, $\alpha = n$: ions)
T_e	= total electron temperature
$T_{e\parallel}$	= electron temperature along $\mathbf{B}$
$T_{e\perp}$	= electron temperature perpendicular to $\mathbf{B}$
$T_{e\top}$	= electron temperature perpendicular to the wall

*PhD student, Division of Magnetised Plasma, jan.miedzik@ipplm.pl.
†Research ssistant, Division of Magnetised Plasma, serge.barral@ipplm.pl.
‡R & D engineer, Space Engines Division, stephan.zurbach@snecma.fr.

$u_\parallel$ = guiding center velocity along **B**
$v_\perp$ = electron velocity in the drifting frame
v_i = ions velocity along **B**
α = angle between the normal to the wall and **B**
δ = SEE yield
δ_e = elastic backscattering electron emission yield
δ_r = inelastic backscattering electron emission yield
δ_{ts} = true SEE yield
$\mathscr{E}_\parallel$ = total electron energy along **B**
$\mathscr{E}_\perp$ = total electron energy perpendicular to **B**
ζ = field line curvilinear coordinate
κ = Boltzmann constant
μ = electron magnetic moment, $\mu \equiv \frac{1}{2} m_e v_\perp^2 / B$
$\Phi_{bi,o}$ = potential barrier of the wall sheath

I. Introduction

Plasma-surface interactions play a crucial role in the operating parameters, efficiency and lifetime of a number of plasma devices. Surface properties such as secondary electron emission yield and material electrical conductivity affect the plasma temperature, sheath potential and electrons/ions energy distribution function (EEDF, IEDF). Insulating walls, which readily acquire a net charge when immersed into a plasma, modify the EEDF via the formation of an electrical sheath which allows only the most energetic electrons to reach the wall, resulting in a EEDF with a characteristic "cold" tail.[1,2] The presence of a magnetic field that is non-uniform or not normal to the walls further affects plasma-surface interactions, for instance through magnetic gradient forces which additionally modify non-isotropic EEDFs by allowing only electrons with a sufficiently small pitch angle to reach the wall.

In Hall thrusters and related devices such as HEMP and CHT, an external magnetic field is imposed which, besides from improving electron confinement, protects the walls from excessive plasma fluxes that are responsible for wall erosion. Experiments have demonstrated the possibility to achieve very low ion beam divergence by modifying the magnetic field of a P5 Hall thruster[3] which according to earlier measurements[4] and numerical simulations[5] was initially characterized by a large beam divergence.

The optimization and physics related to the magnetic field in Hall thrusters, remains, however, only partially understood. The present work contributes to the ongoing research in this field by analyzing the effect of tilted magnetic field lines on the wall-induced conductivity and on plasma properties. This effect is studied by means of one dimensional Particle-In-Cell, model using a guiding center (GC) approximation for electrons motion (PIC-GC electrons, PIC ions) along a single magnetic field line on which, plasma quasineutrality is assumed.[6]

A parametric study was performed which shows that the change in the angle between magnetic field line and wall influences electrons transport across magnetic field lines in a non-trivial manner (Fig. 9).

II. Physical and numerical model

The 1D model is based on the Particle in Cell technique. Electrons motion is approximated by guiding centers, and when needed the angular position is recovered from magnetic momentum (adiabatic invariant). It is

allowed for magnetic field line to intercept non-perpendicularly with the wall, and a fast probabilistic scheme was implemented to generate a random gyrophase upon impact having account for the non-uniformity of the gyrophase probability when filed lines are tilted. The electric field is computed self-consitently applying a modified inertia-less Ohm equation. In order to force the ions flux to the walls within the quasineutral assumption, Bohm condition is implemented.

A. Particle motion and electric field

The equation for the guiding center of an electron in crossed magnetic and electric fields (B_r, E_z) can be written at the leading orders as follows,

$$m_e \frac{du_\parallel}{dt} = -eE_\parallel - \mu \frac{dB}{d\zeta},$$

$$\mathbf{u}_\perp = \mathbf{v}_E \equiv \frac{\mathbf{E}\times\mathbf{B}}{B^2}.$$

Considering the model is 1D(ζ,t) ions are constrained to move along magnetic field line and their equation of motion is $du_i/dt = eE_\parallel/m_i$.

For Hall thruster plasmas, the characteristic gradient lengths are typically much greater than the Debye length so it is rationale to assume quasineutrality. This assumption allows the substitution of Poisson equation by Ohm law to calculate the electric field. On its own, however, the canonical Ohm law does not naturally impose a coupling between ions and electrons densities . In order to achieve such coupling,, the inertial term is dropped and the electrons density in the equation is replaced by ions density, which leads to the equation

$$-eE_\parallel = \frac{|B|}{n_i}\frac{\partial}{\partial\zeta}\left(\frac{n_i \kappa T_{e\parallel}}{|B|}\right) + \bar{\mu}\frac{\partial|B|}{\partial\zeta} + \nu_e m_e u_{e\parallel}. \quad (1)$$

This equation is further simplified by dropping the collision term since $u_{e\parallel}$is typically very small (of the order of v_i) and the collision frequency is typically much less than the bouncing frequency between limiting walls.

B. Tilted magnetic field lines

In the GC approximation of electrons motion, the velocity vector is reduced to its component along the magnetic field line and to the magnetic momentum, which is a constant of motion in slowly varying fields. Upon collision at the boundaries, the full velocity vector must be reconstructed to determine whether the energy perpendicular to the walls is small enough for the electron to be reflected on the sheath or whether it overcomes the sheath barrier and impinges thewall. For the case with magnetic field perpendicular to the wall, the determination of the azimuthal position of electrons is simple. The electron gyro-phase is equiprobably distributed in the $[0, 2\pi]$ interval, and the generation of a single random number is required. The determination of kinetic state is less trivial for oblique field lines, in which case a Keppler-type equation $\Psi = \phi - \left(\frac{v_\perp}{v_z}\tan\alpha\right)\sin\phi$ has to be solved.[6]

C. Secondary electron emission (SEE) model

The main assumptions of the secondary electrons emission model (see details in Ref.[6]) are the following: absorption, inelastic and elastic backscattering on the wall, true secondary electrons creation are allowed; the total energy of all secondary electrons cannot exceed the energy of the primary electron; the total energy of all secondary electrons is sampled uniformly in the interval $[0, E_0]$ where E_0 is the primary electron

energy; the energy of elastically backscattered electrons remains unchanged after collision; the energy of inelastically backscattered electrons is sampled from a Maxwellian flux distribution truncated at a constant temperature of 5 eV; the angular distribution of inelastically backscattered and true secondary electrons follows a cosine law;[7] the angular dependence of the SEE yield on the primary electrons is neglected. Although the authors are not aware of experimental data regarding the angular dependence of the SEE, the last assumption appears reasonably justified by the high porosity of ceramic walls and their polycrystalline structure.

D. Bohm criterion

The quasineutrality assumption makes it necessary to impose a suitable boundary condition that accounts for the physics within the wall sheath. The so called Bohm condition is implemented and the electric field in boundary cells is calculated as follows:[6]

$$E_{\parallel} = \frac{2}{e\left(\zeta_w - \langle\zeta\rangle_{cell}\right)}\left(T_{e\parallel} - \left\langle v_i^2\right\rangle_{cell} m_i\right) . \tag{2}$$

III. Simulation

A. Parameters and numerical methods

Computations were performed for one magnetic field line with the spatial dependence shown in the Fig. 1. A normalized magnetic field B^* defined as $B/E_{\perp}$ was introduced. The domain is bounded by walls at positions $\zeta = -1\,\mathrm{cm}$ and $\zeta = 1\,\mathrm{cm}$. The simulation is initialized with a large number of particles in order to minimize statistical noise. At the initial moment, electrons are in Maxwellian equilibrium at a constant temperature $T_{e0} = 3\mathrm{eV}$ whereas the temperature of ions is set to $T_{i0} = 2000K$. The density of neutrals is constant in time and space during the simulation. The time step for electrons is constrained by the CFL condition $\Delta t = CFL * \Delta\zeta / v_{\parallel \max}$ for ions, the time stepis kept at 5 times this value at most to warrant stability. The influence of tilted magnetic field lines is assessed from a set of simulations that considered incidence angles ranging from -80° up to 80° every 10°. The incidence angle is changed by tilting the walls as shown in Fig. 3, since this method ensures that the length of the magnetic field line remains constant across simulations. Note, however, that for the model at hand, tilting the walls is exactly equivalent to using a curved magnetic in conjunction with parallel walls provided that the incidence angle with the walls and the field line length are preserved.

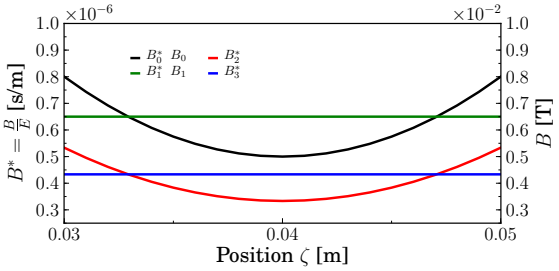

Figure 1: Magnetic field and normalized magnetic field strength.

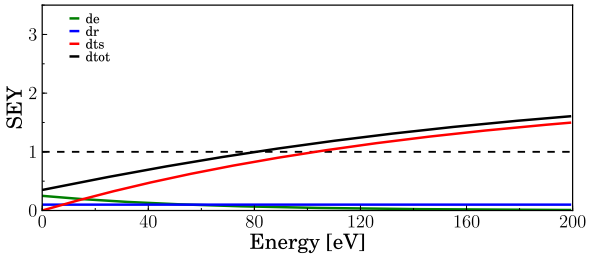

(a) First cross-over energy 80eV

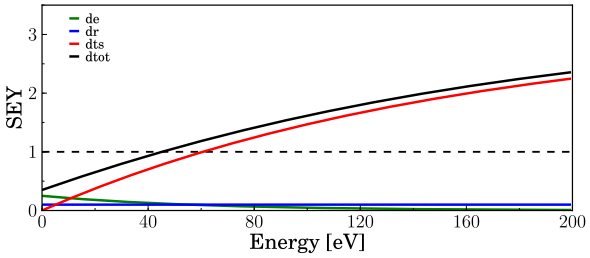

(b) First cross-over energy 45eV

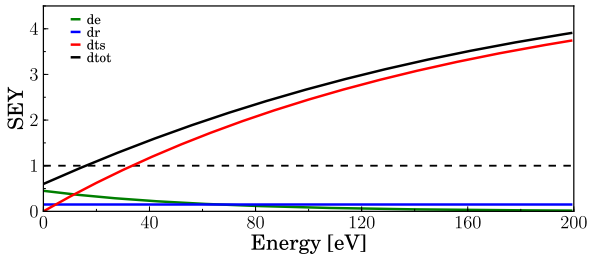

(c) First cross-over energy 15eV

Figure 2: Secondary electron emission functions considered in simulation.(a)I SEE. (b) II SEE. (c) III SEE

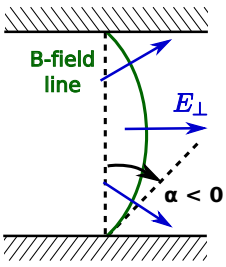

(a)

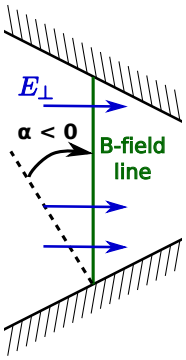

(b)

Figure 3: (a) Typical geometry of a B-field line in Hall thrusters and (b) approximate problem solved in the GC-QPIC simulation.

B. Simulation results

1. *Secondary electron emission influence*

The influence of secondary electrons emission on the plasma properties is assessed by a set of simulations run for normalized magnetic field B_2^* and for all considered incidence angles. The SEE profiles are given in Fig. 2. As shown in Fig. 4, provided that the first cross-over energy is sufficiently high, SEE does not noticeably influence plasma temperatures. Once the first cross-over energy is close to the energy gained by electrons in the cross fields after a collision, the electrons temperature $T_{e\|}$ and the normalised sheath potential of Fig. 5 are both influenced.

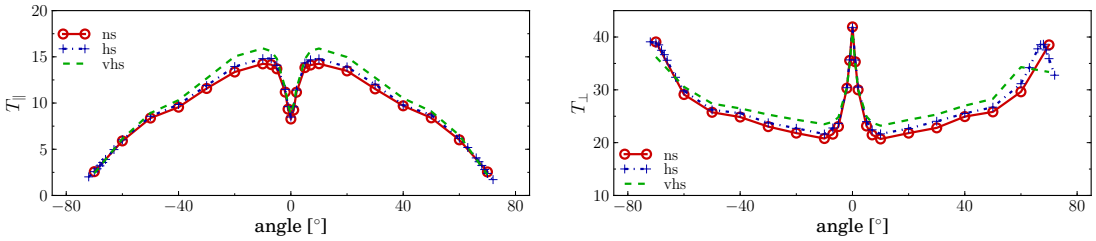

Figure 4: SEE influence on $T_{e\|}$ (left) and $T_{e\perp}$ (right) in boundary cells for magnetic field B_2^*.

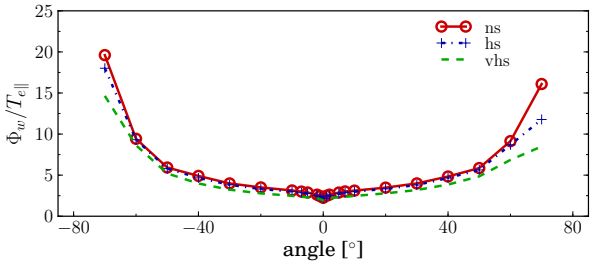

Figure 5: SEE influence on the normalized sheath potential (potential normalized by $T_{e\|}$ in boundary cells) for magnetic field B_2^*.

2. *Influence of the magnetic field lines incidence angle*

The influence of olbique magnetic field lines on the plasma parameters and cross-field drift of electrons was determined by a parametrical study performed for various normalized magnetic field and two different secondary electrons emission profiles.

One of the most immediate observation is that the inclination of the magnetic field has a great influence on temperature isotropy. As show in Fig. 6 $T_{e\perp}$ decreases when the magnetic field lines becomes non-perpendicular to the wall. This is a direct consequence of the fact that, for non-perpendicular field lines, each electron collision on the sheath changes the direction of the velocity vector, thereby transferring energy from the perpendicular to the parallel direction, resulting in a decrease of temperature anisotropy (Fig. 7). Interestingly, when field lines become nearly parallel to the walls, the anisotropy increases again, which is most obvious in the two configurations I SEE+B_3^* and II SEE+B_2^*, and is more marked when the**B** field configuration is ion-focussing. It is surmised that the mechanism responsible for this is that, upon reaching the walls, the electrons are re-emitted according to a cosine law which privileges the direction normal to the wall. After being accelerated by the sheath (perpendicularly to the wall) and injected back into the plasma bulk, nearly all energy that was distributed between the $\perp$ and $\|$ directions before the collision is

now confined in the direction normal to the wall, which in such configuration is almost perpendicular to the **B** field line and therefore only contributes to $T_{e\perp}$.

The change in α also influences the sheath potential as can be seen in Fig. 8. As the angle changes from 0° to 40°, the sheath potential increases monotonically together with the temperature normal to the wall, $T_{e\top} = \cos^2(\alpha) * T_{e\perp} + \sin^2(\alpha) * T_{e\|}$. For all three α angles, the EVDF is truncated. For $\alpha = 0^\circ$, a clear correaltion can be established between the change in slope of the distribution and the wall potential. Most electrons with energy along the magnetic field greater than the wall potential are cooled down at the walls or absorbed. Electrons emitted from the walls have an energy in the direction perpendicular to the wall barely above the sheath potential.

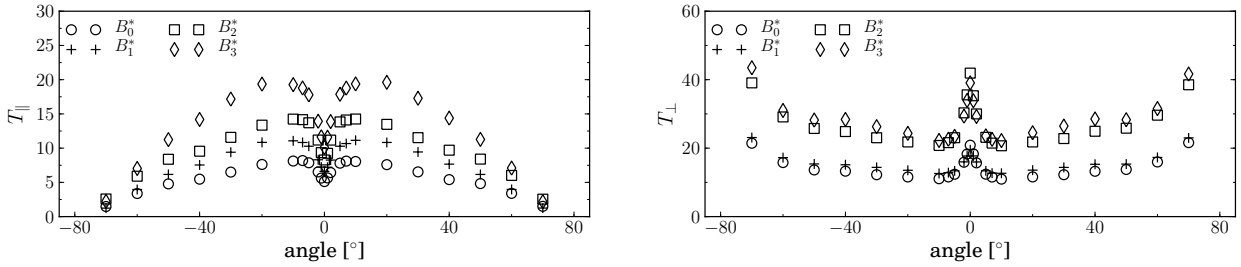

(a) (b)

Figure 6: Temp erature parallel (left) and perpendicular (right) to the **B** field line as a function of magnetic field line angle incidence.

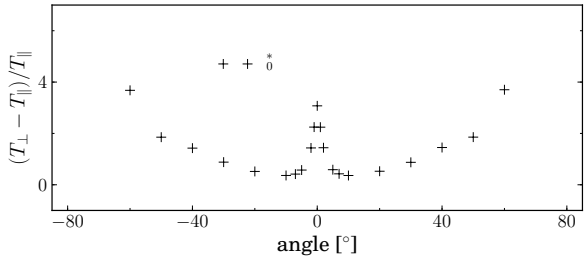

Figure 7: Relative electron anisotropy degree $\frac{T_{e\perp}-T_{e\|}}{T_{e\|}}$ in the bounding cell as a function of magnetic field line angle.

Changes in the incidence angle of the magnetic field line influence also heavily the electrons cross-field drift (see Fig. 9). Electrons travel to the anode with the highest (resp. lowest) velocity for ion focusing (resp. defocusing) magnetic field topologies. This behaviors stems from the combination of two phenomena. First, the ion focusing topology privileges electron collisions on the high potential side of the flux tube as this side lies closer to the wall, meaning that such electrons are in general at a higher potential than their guiding upon impact. Second,electrons colliding with the wall in this configuration are in general close to the maximum energy of their cycloidal trajectory and thus yield more secondary electrons (see Fig. 10). Secondary electrons are thereafter accelerated towards anode by the electric field $E_\perp$ and contribute to the cross-field drift.

Finally, the influence of the electric field $E_\perp$ was assessed (Fig. 11). Changes in the electric field have, expectedly, a great influence on the cross field drift. Higher $E_\perp$ translate into higher drift velocity $E \times B$ andthus higher energy upon collision, as well as larger Larmor radii and therefore faster collisional transport to the anode.

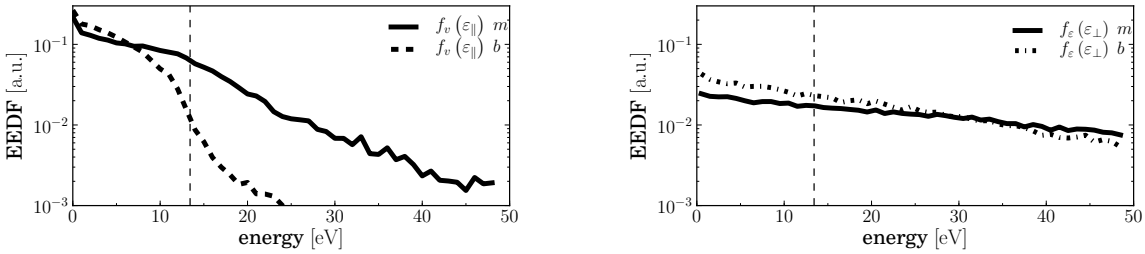

(a) Incidence angle 0° (B perpendicular to the walls)

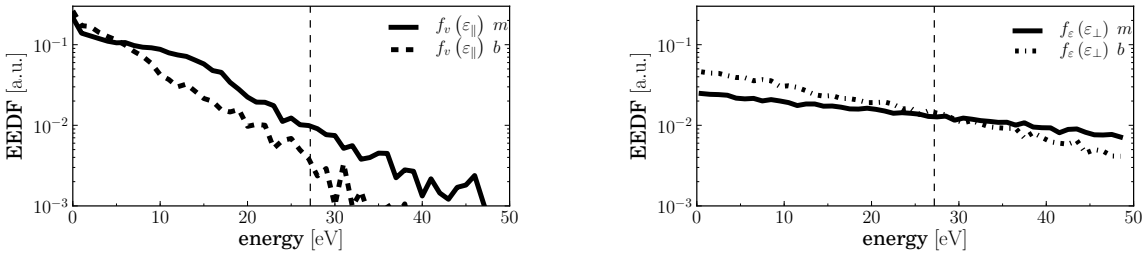

(b) Incidence angle 40°

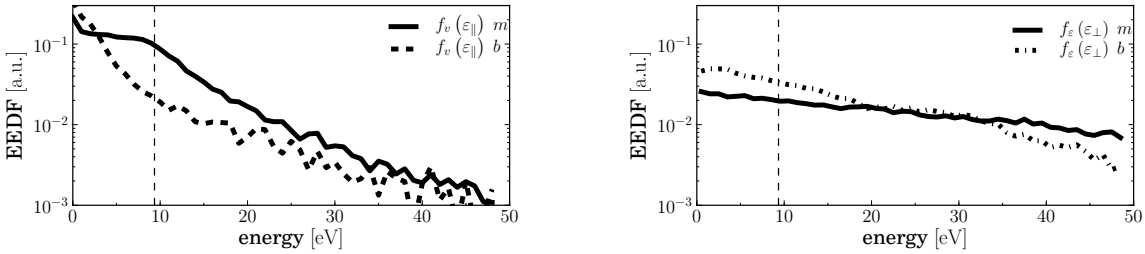

(c) Incidence angle 80°

Figure 8: Computed EEDF for $\mathscr{E}_\perp$ and EVDF for $v_\parallel$ for three different incidence angles, magnetic field B_0^* and SEE 2c. The continuous line is the distribution in the middle of the computational domain and the dashed line is the distribution in boundary cells. The vertical line is the value of the sheath potential at the walls.

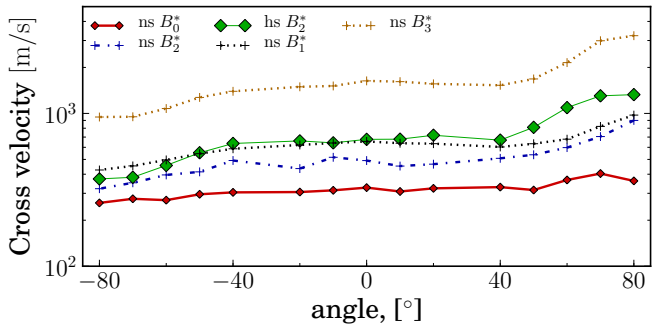

Figure 9: Average cross-field drift velocity of electrons towards anode as a function of the magnetic field tilt angle. A positive angle indicates an ion focusing topology, with a zero angle corresponding to a magnetic field normal to the walls.

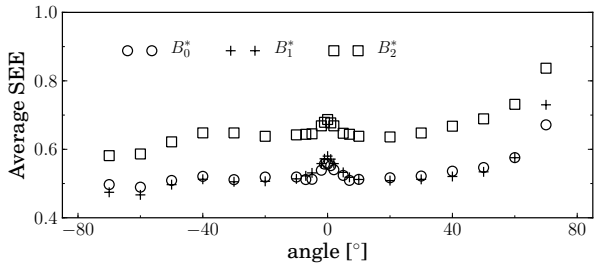

(a)

Figure 10: Average SEE in function of magnetic field line angle

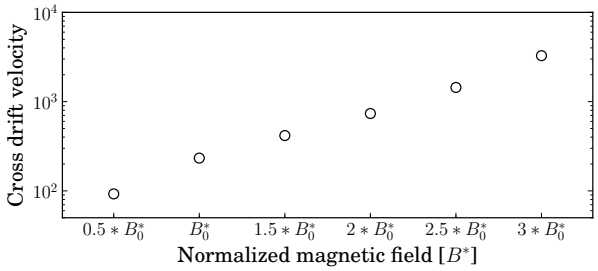

Figure 11: Cross drift velocity as a function of $E_\perp$ for incidence angle 0° (note the logarithmic scale). Changes in $E_\perp$ can be also viewed as a change in normalized magnetic field B^*. The magnetic profile B_0 plotted on Fig. 1 was used.

IV. Conclusion

It is found that highly ion focusing topologies result in a greater probability for electrons to collide with the walls on the high energy side (high potential side) of the magnetic flux tube. Consequently, such geometry tends to increase the guiding center shift in the cross-field direction upon collision and thus the wall-induced electron transport. The opposite effect is observed for ion-defocussing topologies. At the same time, it is shown that oblique **B** field lines affect the sheath potential and strongly decreases temperature anisotropy because in such case, transfers of energy between the $\parallel$ and $\perp$ directions are possible even during specular reflection of electron on the sheath, which is by far the most frequent type of collision. This contrasts with the case of a magnetic field normal to the wall, where specular reflection on the wall sheath conserve energy in the $\parallel$ and $\perp$ and directions. Additionally it is demonstrated that, due to the relatively high anisotropy of electron energy, magnetic mirroring improves insulation of the plasma from the wall in a sizable manner and results in a decrease of both the sheath barrier potential and of the wall-induced electron mobility.

Acknowledgments

J. Miedzik is grateful to Snecma for the sponsorship of his PhD thesis.

This work has been performed with funding from the French Research Group “Propulsion par Plasma dans l’Espace” (GDR 3161 CNRS/CNES/SNECMA/Universités).

References

[1]Jolivet, L. and Roussel, J.-F., "Effects of the Secondary Electron Emission on the Sheath Phenomenon in a Hall Thruster," *Proc. 3rd International Spacecraft Propulsion Conference*, Cannes (France), 2000, p. 367.

[2]Meezan, N. B. and Cappelli, M. A., "Kinetic Study of Wall Collisions in a Coaxial Hall Discharge," *Phys. Rev. E*, Vol. 66, 2002, pp. 036401.

[3]Linnell, J. A. and Gallimore, A. D., "Internal Plasma Potential Measurements of a Hall Thruster Using Plasma Lens Focusing," *Phys. Plasmas*, Vol. 13, No. 10, 2006, pp. 103504.

[4]Haas, J. M. and Gallimore, A. D., "Internal Plasma Potential Profiles in a Laboratory-Model Hall Thruster," *Phys. Plasmas*, Vol. 8, No. 2, 2001, pp. 652.

[5]Keidar, M., Gallimore, A. D., Raitses, Y., and Boyd, I. D., "On the Potential Distribution in Hall Thrusters," *Appl. Phys. Lett.*, Vol. 85, No. 13, 2004, pp. 2481–2483.

[6]Miedzik, J., Barral, S., and Zurbach, S., "Study of Plasma Confinement by Magnetic Fields in Hall Thrusters using Quasi-Neutral PIC Modeling," *Proc. 32nd International Electric Propulsion Conference*, No. 11-238, The Electric Rocket Propulsion Society, Worthington, OH, Wiesbaden (Germany), 2011.

[7]Greenwood, J., "The Correct and Incorrect Generation of a Cosine Distribution of Scattered Particles for Monte-Carlo Modelling of Vacuum Systems," *Vacuum*, Vol. 67, 2002, pp. 217.